Evaluating Statistical Consistency in the Ocean Model Component of the Community Earth System Model (pyCECT v2.0)

A. H. Baker[1], Y. Hu[2,3], D. M. Hammerling[1], Y. Tseng[1], H. Xu[1], X. Huang[2,3], F. O. Bryan[1], and G. Yang[2,3]

[1]The National Center for Atmospheric Research, Boulder, CO, USA
[2]Center for Earth System Science,Tsinghua University, 100084, China
[3]Joint Center for Global Change Studies, Beijing, 100875, China

Correspondence to: Allison H. Baker (abaker@ucar.edu)

Abstract. The Parallel Ocean Program (POP), the ocean model component of the Community Earth System Model (CESM), is widely used in climate research. Most current work in CESM-POP focuses on improving the model's efficiency or accuracy, such as improving numerical methods, advancing parameterization, porting to new architectures, or increasing parallelism. Because ocean dynamics are chaotic in nature, achieving bit-for-bit (BFB) identical results in ocean solutions cannot be guaranteed for even tiny code modifications, and determining whether modifications are admissible (i.e. statistically consistent with the original results) is non-trivial. In recent work, an ensemble-based statistical approach was shown to work well for software verification (i.e., quality assurance) on atmospheric model data. The general idea of the ensemble-based statistical consistency testing is to use a qualitative measurement of the variability of the ensemble of simulations as a metric with which to compare future simulations and make a determination of statistical distinguishability. The capability to determine consistency without BFB results boosts model confidence and provides the flexibility needed, for example, for more aggressive code optimizations and the use of heterogeneous execution environments. Because ocean and atmosphere models have differing characteristics in term of dynamics, spatial variability, and time-scales, we present a new statistical method to evaluate ocean model simulation data that requires the evaluation of ensemble means and deviations in a spatial manner. In particular, the statistical distribution from an ensemble of CESM-POP simulations is used to determine the standard score of any new model solution at each grid point. Then the percentage of points that have scores greater than a specified threshold indicates whether the new model simulation is statistically distinguishable from the ensemble simulations. Both ensemble size and composition are important. Our experiments indicate that the new POP ensemble consistency test (POP-ECT) tool is capable of distinguishing cases which should be statistically consistent with the ensemble and those which should not, as well as providing a simple, subjective and systematic way to detect errors in CESM-POP due to the hardware or software stack, positively contributing to quality assurance for the CESM-POP code.

1 Introduction

The Community Earth System Model (CESM) is a popular and fully-coupled climate simulation code (Hurrell et al., 2013) that regularly contributes to the Intergovernmental Panel on Climate Change (IPCC) assessment reports (e.g., Stocker et al., 2013). CESM consists of multiple component models that are coupled together, including component models for the atmosphere,

ocean, sea ice, and land. Here, we focus on the Parallel Ocean Program (POP) component of CESM, an extension of the ocean general circulation model originally developed at Los Alamos National Laboratory (Smith et al., 2010). The CESM-POP solves the three-dimensional (3D) primitive equations for ocean dynamics with hydrostatic and Boussinesq approximations, representing ocean processes across a broad range of spatial and temporal scales. Much new development in CESM-POP is aimed at reducing computational costs (e.g., Hu et al., 2015), but ongoing development of any type in a simulation code requires software quality assurance to ensure that no errors are introduced. The need for some sort of quality assurance to maintain confidence in the science results is particularly critical for climate models whose simulation output may influence policy decisions with broad societal impact (Carson, 2002; Easterbrook et al., 2011).

Climate models such as CESM are generally large and complex, and the plethora of model configuration options makes them difficult to test exhaustively (Clune and Rood, 2011; Pipitone and Easterbrook, 2012). Further, because of the chaotic nature of climate models, determining whether a difference in simulation results is due to an error or simply to the model's natural variability can be challenging. Note that a roundoff-level perturbation added to an initial condition or intermediate result can lead to sizable differences in the final result. New developments in CESM-POP, particularly those aimed at improving performance (such as taking advantage of new heterogeneous computing technologies or improving numerical methods), typically result in data output that is not bit-for-bit (BFB) identical to the original code. For CESM-POP, even selecting a different number of cores on the same architecture results in non-BFB identical output. The ability to directly evaluate climate consistency in the CESM-POP ocean data facilitates the advancement of the code development in general and enables the flexibility to take advantage of new computing (hardware and software) technologies.

The CESM ensemble consistency test (CESM-ECT), recently developed in Baker et al. (2015), addresses the difficulty in comparing climate model outputs via a new ensemble-based tool that evaluates whether a new climate run (e.g., resulting from a hardware or software modification) is statistically distinguishable from an "accepted" ensemble of original (unmodified) runs. However, the CESM-ECT tool presented in Baker et al. (2015) only evaluates variables from the Community Atmosphere Model (CAM) component of CESM, and the experimental runs do not use a fully-coupled CESM configuration (i.e., rather than POP, the ocean component is the Climatological Data Ocean Model, which contributes sea surface temperature data but does not respond to forcing from the atmosphere component). For clarity, we refer to the general ensemble statistical consistency testing approach for CESM as CESM-ECT. We denote the methodology applicable to the Community Atmospheric Model component by CAM-ECT, which is a module in the CESM-ECT suite of tools that we are developing. We note that applying the CAM-ECT methodology "as is" directly to ocean data is not feasible because the ocean and atmosphere models greatly differ in terms of their dynamics, spatial scales and time scales. For example, the synoptic scale in the ocean dynamics is one to two orders of magnitude smaller than that in the atmosphere, and the propagation time scale for adjusting the ocean is many orders of magnitude slower than that in the atmosphere, particularly for the deep ocean. Therefore, we have developed a new approach to provide an ocean-specific methodology for statistical consistency testing, which we denote POP-ECT. Although the new POP-ECT tool is similarly based on using an ensemble of CESM simulations to gauge model variability, it is distinct from CAM-ECT in that the statistical process does not use global means but instead takes spatial patterns of differing variability into account in the ocean due to a larger time to reach the global quasi-steady state in the ocean than the atmosphere. Further,

the smaller number of diagnostic variables available from the ocean model (as compared to the atmosphere where over one hundred variables are considered) allows for a different approach as well. However, like CAM-ECT, POP-ECT is intended for software quality assurance, and a specific model setup is used to catch potential errors in the hardware of software stack, for example, when porting to a new machine, after a code modification, or in general when non-BFB identical results and a

5 consistant climate are both expected. The CESM-ECT tools are not intended as a substitute for appropriate unit testing (nor to detect errors in cases where results that should be BFB are not). Finally, note that all experiments in this paper use the publicly available CESM 1.2.2 release.

This paper is organized as follows. The background information is reviewed and discussed in Sect. 2. In Sect. 3, we introduce the new statistical consistency testing methodology for ocean model data, referred to as POP-ECT, as well as the necessary

10 software tools. We evaluate the approach and explore the effect of the simulation length with experimental tests in Sect. 4. Finally, we explore the new approach's sensitivity to ensemble size in Sect. 5 and provide concluding remarks in Sect. 6.

2 Background discussion

2.1 Current ocean model quality assurance testing

The current POP-specific quality assurance test, referred to as POP-RMSE, is a simple test that is intended to evaluate whether

15 the CESM-POP code was successfully ported to a new architecture and aims to discover issues related to a new machine's hardware or software stack. This test consists of running five days of a specified case on a new machine and then comparing the output to that of a standard dataset released by the National Center for Atmospheric Research (NCAR). The comparison is done only for the sea surface height (SSH) field via a root-mean-square error (RMSE) calculation, which measures the difference between the two datasets, X_0 and X_1, each containing n grid point values:

20 $$RMSE(X_0, X_1) = \sqrt{\frac{1}{n}\sum_{i=1}^{n}(X_1(i) - X_0(i))^2}.$$

The rate of growth of RMSE was compared to the growth between two reference cases in which the convergence criteria for the solver was changed by one order of magnitude.

The simple methodology in POP-RMSE is convenient for evaluating CESM output on a new machine, but it is far less comprehensive than CAM-ECT for atmospheric simulation data. For example, POP-RMSE was unable to quantify the small

25 climate state changes due to recent linear solver modifications in CESM-POP in Hu et al. (2015). In Hu et al. (2015), the authors replaced the default preconditioned conjugate gradient (PCG) solver for the barotropic mode of POP by an alternative preconditioned Chebyshev-type iterative (P-CSI) solver to enhance the computational performance. While the P-CSI solver had considerably lower communication costs for high-resolution simulations than PCG, showing that the use of an alternative solver did not negatively impact the ocean simulation results was critical for acceptance. Therefore, in Hu et al. (2015), to gauge

30 the effectiveness of the POP-RMSE test in detecting solver differences over time, monthly data was collected for 36 months from a CESM-POP $1°$ resolution case with multiple convergence tolerances between 10^{-10} and 10^{-16}. Figure 1 displays the

RMSE between the strictest case (10^{-16}) and the other tolerances listed in the figure's legend for the temperature field. Despite the range in convergence tolerances used, Fig. 1 gives scant evidence of any solver-induced error (Hu et al., 2015).

2.2 Ensemble consistency testing with CESM-POP

Because the RMSE approach did not elucidate differences between convergence tolerances, Hu et al. (2015) adapted the ensemble approach that was initially described in the context of atmospheric data compression in Baker et al. (2014) (a precursor to the CESM-ECT approach) for CESM-POP data. In particular, Hu et al. (2015) created an ensemble consisting of 40 runs of 36 months in length that differed by an $\mathcal{O}(10^{-14})$ perturbation in the initial ocean temperature field. Next the root-mean-squared Z-score between the new case, $\tilde{X}$, and the ensemble of test cases was calculated as follows. If size of ensemble E is denoted by N_{ens}, then at each grid point i, N_{ens} values exist for each variable X. The average and standard deviation at each grid point i for the N_{ens} ensemble members of E are denoted by μ_i and σ_i, respectively. Recalling that n is the number of grid points, for each variable $\tilde{X}$ in the new run, the root-mean-square Z-score of $\tilde{X}$ as compared to ensemble E is

$$RMSZ(\tilde{X}, E) = \sqrt{\frac{1}{n}\sum_{i=1}^{n}(\frac{\tilde{x}_i - \mu_i}{\sigma_i})^2}. \tag{1}$$

Figure 2 shows the results of the RMSZ scores for the same five selected convergence tolerances as in Fig. 1, and now the error induced by the least strict tolerances is more evident. Based on this result in Fig. 2, Hu et al. (2015) evaluated the suitability of a new solver in CESM-POP.

2.3 Ensemble consistency testing for the Community Atmosphere Model

The CESM-ECT approach presented in Baker et al. (2015) uses an ensemble to quantify the natural variability of the CESM model's climate and then compares new simulations (resulting from a software, hardware, or non-BFB change) against the ensemble distribution. The key idea is that if the output data from a new simulation is not statistically distinguishable from the ensemble of runs, then the new run is deemed "consistent". Statistical consistency is a key ingredient in the quality assurance aspect of model code verification (Oberkamf and Roy, 2010). The CESM-ECT approach was first applied to history output from the Community Atmosphere Model (CAM) component, resulting in the CAM-ECT tool. CAM data were a logical first target as the time scales for changes to propagate throughout the atmosphere are shorter compared to other CESM components and CAM contains a large number of independent variables that cover the whole globe.

As described in Baker et al. (2015), the ensemble for CAM-ECT is created on a trusted machine with an accepted version and configuration of CESM. The ensemble consists of 151 simulations of 1-year in length that differ only in a random perturbation of the initial atmospheric temperature field of $\mathcal{O}(10^{-14})$. The output data contains only the annual averages at each grid point for the number of specified variables from CAM, denoted by N_{var}, which represent whole atmospheric fields (by default, $N_{var} = 120$). The CAM-ECT tool creates a statistical distribution that characterizes the ensemble using principal component analysis (PCA) on the global area-weighted mean distributions for each variable across the ensemble. The distribution of principal component (PC) scores are retained for comparison with new simulation runs. A small set of new runs (generally

3) either passes or fails based on the number of PC scores that fall outside a specified confidence interval (typically 95%). Parameters specifying the pass/fail criteria can be tuned to achieve a desired false positive rate for the test.

2.4 Motivation

While the solver verification work in Hu et al. (2015) was illuminating and adequate for the task at hand, it prompted several questions that motivated our work to develop a more comprehensive technique such as CAM-ECT for evaluating CESM-POP data. First, a key consideration for a more general POP verification tool was the concern over spatial variability in the ocean, which is much more pronounced than in the atmosphere. Both CAM-ECT as well as the RMSZ strategy in Hu et al. (2015) evaluate the differences in terms of spatial averages, and it was unclear whether this approach would be sufficient to detect any accuracy issue or model error in the ocean. Second, because CESM-POP has fewer independent diagnostic variables than the CAM, we re-visit the question of appropriate metrics for consistency evaluation. Third, the selection of different metrics prompted further examination of the appropriate ensemble size. While an ensemble of size 40 ensemble was sufficient for detecting linear solver errors in Hu et al. (2015), this dimension was not thoroughly explored in a more general context, particularly in light of the recommended ensemble size of 151 for CAM-ECT. Finally, the difference in temporal scales between the ocean and atmosphere prompted us to investigate the required length of ensemble runs. Because the time-scales in the ocean are slower than in the atmosphere, intuitively a longer ensemble length is needed for statistical consistency testing with CESM-POP. Note, though, that the initial results in Fig. 2 suggest that this presumption may not be true. The RMSZs continue to decrease with time after a few months when the tolerances are small enough (i.e., tolerance is smaller than 10^{-12}), suggesting the required length of simulation merits further investigation. In fact, Fig. 2 shows that this particular 1-degree ocean data is relatively deterministic and the initial differences begin to damp out (grow) after the first year when the tolerances are small (unrealistically large).

3 A new statistical consistency test for POP

Expanding the CESM-ECT suite to include a consistency test for CESM-POP, which we denote POP-ECT, data requires determining an appropriate ensemble to represent ocean model variability and developing a methodology to address ocean-specific characteristics. We first discuss the ensemble creation. We then describe the new testing procedure.

3.1 POP ensemble construction

We evaluate whether differences in CESM-POP output data are statistically significant (i.e., indicative of a changed climate state) by comparing to an ensemble of simulations representing an accepted ocean state. Therefore, the first stage in applying the CESM-ECT approach to CESM-POP data is creating an appropriate ensemble. Clearly, the ensemble composition is critical to an effective test, and simulations should be produced on an accepted machine with an accepted version of CESM. Note that as compared to CAM, the ocean model has fewer independent diagnostic variables: temperature (TEMP), sea surface height

(SSH), salinity (SALT), and the zonal and meridional velocities with respect to the model grid (UVEL and VVEL, respectively). Of these five variables, SSH is 2D and the remainder are 3D.

For POP-ECT, we create an ensemble E of N_{ens} simulations, denoted by $E = \{E_1, E_2, \ldots, E_{N_{ens}}\}$, that differ only by an $\mathcal{O}(10^{-14})$ perturbation to the initial ocean temperature field. This initial perturbation size is on the order of double-precision round-off error and should not be climate-changing. The size of the ensemble must be sufficient to create a representative distribution, but as small as possible to avoid high computational cost. While we address in detail our choice of ensemble size later in Sect. 5, we use $N_{ens} = 40$ for the discussion in this section and the experiments in the next. Our experiments indicate that this choice of ensemble size adequately represents the natural variability in the ocean for testing purposes. The ensemble simulation data consists of monthly temporal averages at each grid point i for the 5 POP diagnostic variables: TEMP, SSH, SALT, UVEL, and VVEL. Each of these variable datasets X contains N_X grid points and is denoted by $X = \{x_1, x_2, \ldots, x_{N_X}\}$, where x_i is a scalar monthly average at grid point i. Data is collected for T months (i.e., T time slices of monthly data).

The next step in CESM-ECT approach is to characterize the ensemble distribution in a qualitative way to facilitate the evaluation of new runs. This statistical description of the ensemble is stored in a so-called ensemble summary file and is associated with the CESM softare tag used to generate the ensemble simulations. The history files from the N_{ens} simulations do not need to be retained once the summary file has been created. Recall that for CAM data, CAM-ECT calculates the global weighted-area mean for each variable from the annual temporal averages available at each grid point. This calculation results in a distribution of N_{ens} global means for each variable. However, this approach of using global weighted-area means will not be appropriate for ocean model data, as ocean variability is less heterogeneous across the grid than atmospheric data.

For example, consider an ensemble of $N_{ens} = 40$ CESM simulations with a $1°$ resolution CESM-POP grid run for $T = 36$ months. In Fig. 3, we show spatial plots of the standard deviations of the sea surface temperature (SST), across the ensemble members after 1, 12, 24, and 36 months. Note that the SST is simply the top layer of the 3D variable TEMP (more precisely, the top 10 meters of upper ocean). Figure 3 shows that the standard deviation is far from heterogeneous with orders of magnitude differences across the grid (see the color bar scale). Also notable is the change from 1 month to 12 months associated with the model instability associated with the development of hydrodynamic instability of the flow as the model spins up. At the end of one year, the larger standard deviation in the tropical regions suggest a larger uncertainty due to the growth of tropical instability waves (Legeckis, 1977) in the ensembles. The large variability can be easily enhanced in the equatorial regions because of the finer resolution in the tropics (approximately $1/3°$). There are also some pools of large standard deviation in the downstream of the major ocean current systems. The change from 12 months to 36 is more subtle, indicating the associated physical instability may not grow further due to the ocean dissipation. Given the range in variability evident in Fig. 3, the RMSZ score strategy as used for verification in Hu et al. (2015) (and discussed in Sect. 2) may include the uncertainty introduced by the actual physical instability in regions with large variability (e.g., the equatorial Pacific) and may unnecessarily flag potential errors in regions with little to no variability due to the denominator in Eq. (1). Note the range of variability shown in Fig. 3 is certainly resolution dependent, and the results in Fig. 3 are specific to the rather dissipative low-resolution ocean model (e.g., $1°$ CESM-POP) used in most climate studies.

Therefore to create an ensemble statistical consistency test that is robust for CESM-POP data, we must create a distribution describing the ensemble that contains spatial as well as temporal information. In particular, POP-ECT creates an ensemble file with T monthly time slices of CESM-POP data that contains:

- $N_{var} \times N_X \times T$ monthly mean values across the ensemble at each grid point i (μ_i)

- $N_{var} \times N_X \times T$ standard deviations of ensemble monthly mean values at each grid point i (σ_i),

which is to say that we retain the ensemble mean and standard deviation at each of N_x grid points (note that N_X depends on whether X is a 2D or 3D variable) for the specified number of months, e.g. $T = 36$.

Finally, we note that without special treatments, the CESM-POP could generate unrealistic salinity distributions in the closed marginal seas because there is no appreciable freshwater feedback between the freshwater and salinity (e.g. Hudson Bay, the Mediterranean Sea). The current CESM-POP has strong freshwater restoring in the marginal seas, and weak restoring elsewhere; a salinity restoring to the Polar Science Center Hydrographic Climatology version 2 (updated from Steele et al. (2001)). These specific treatments can maintain a salinity balance but act as artificial forcings to the model dynamics. Therefore, in this work we do not address the complexity of how to do verification properly in the marginal seas and instead restrict our attention to the open oceans.

3.2 Testing procedure

Given the POP-ECT summary file, we determine whether new simulation output data (e.g. from a code modification, a new machine, a new compiler option) is statistically consistent with the ocean climate categorized by the reference ensemble distribution as follows. We take the approach of evaluating the standardized difference between the ensemble and the new run *at each grid point*. For each grid point i and each new variable $\tilde{X}$, we calculate the distance between $\tilde{X}$ and the ensemble data via a standard Z-score measurement for a given monthly time slice t. In particular, given the values of $\tilde{X}$ at time t, $\tilde{X} = \{\tilde{x}_{1,t}, \tilde{x}_{2,t}, \ldots, \tilde{x}_{N_X,t}\}$, the Z-score at grid point i for variable $\tilde{X}$ at time t is

$$Z_{\tilde{x}_{i,t}} = \frac{\tilde{x}_{i,t} - \mu_{i,t}}{\sigma_{i,t}},$$

where $\mu_{i,t}$ and $\sigma_{i,t}$ are the ensemble mean and standard deviation respectively, at grid point i for variable X at the specified month t as specified in the ensemble summary file.

Now for a particular time slice t, we drop all subscripts t from relevant variables, e.g. the Z-score becomes $Z_{\tilde{x}_i}$. We define an allowable tolerance tol_Z for the Z-score at each point, meaning that if $Z_{\tilde{x}_i} > tol_Z$, then point i is denoted a "failed" point. Recall that a Z-score indicates the number of standard deviations away from the mean, and a large Z-score indicates that the new case is far from its climate state in the ensemble. Next we look at the overall percentage of grid points that have passing Z-scores, defining the Z-score Passing Rate (ZPR) for variable $\tilde{X}$ as:

$$ZPR_{\tilde{X}} = \frac{\#\{i \mid \tilde{x}_i \in \tilde{X} \wedge |Z_{\tilde{x}_i}| \leq tol_Z\}}{\#\{i \mid \tilde{x}_i \in \tilde{X}\}}. \tag{2}$$

To make an overall determination of whether variable $\tilde{X}$ passed, we set a minimum threshold for the ZPR (min_{ZPR}). In particular, if $ZPR_{\tilde{X}} \geq min_{ZPR}$ then variable $\tilde{X}$ passes. By default, the Z-score tolerance is $tol_Z = 3.0$, and the ZPR threshold is $min_{ZPR} = 0.9$. In other words, 90% of the new values for variable $\tilde{X}$ must be within 3.0 standard deviations of the ensemble mean (μ_i) at each grid point i for $\tilde{X}$ to "pass". This process is repeated for all five independent diagnostic variables, and all variables must pass for the overall simulation to be deemed statistically consistent.

Note that the calculated Z-scores change with simulation length. Because of the longer time-scales present in the ocean, we ran the CESM simulations for most of the experiments in the paper for 36-months. In addition, we output monthly time slice data for POP-ECT (as opposed to the annual temporal mean for CAM-ECT) to determine whether the ensemble ocean states stabilize (or not) over time. In addition, for some of the experimental results in this paper, we find it more useful to plot the Z-score failure rate (i.e., $1 - ZPR$) than the ZPR.

As will be evident in the following section, the ZPRs generally become stable after a few months, and the stability trends across the diagnostic variables are similar. Therefore, in addition to picking a suitable Z-score tolerance and passing rate, we choose a checkpoint (t_C) at which to evaluate the new run result (instead of checking at all T months of data). Note that the length of the ensemble simulations does not need to be longer than t_C.

3.3 Software tools

To make our new POP-specific testing methodology accessible to both users and developers, we added POP-ECT to the existing CESM-ECT suite of Python tools (pyCECT v2.0) , which are included in the CESM public releases. The CESM-ECT Python tools include the tools that create the CESM module-specific ensemble summary files as well as pyCECT, which performs the statistical consistency test using the specified ensemble summary file. Because the POP-ECT summary file is distinct from the CAM-ECT summary file, we created the parallel Python code pyEnsSumPop to generate the POP-ECT summary files. In particular, from an ensemble of CESM-POP simulation output files, pyEnsSumPop creates the ensemble summary file (in parallel) containing the ocean model statistics as described in Sect. 3.1. The CESM Software Engineering Group creates a new ensemble of POP simulation data as needed, which currently coincides with the release of a software tag that contains modifications known to alter the climate from the previously tagged version's climate. The appropriate POP-ECT ensemble summary files are included in development and release tags for CESM as noted in Sect. 7. Given a POP-ECT summary file, a user or developer can then evaluate "new" simulation data for consistency using the pyCECT Python tool, which is now able to evaluate results based on either the POP-ECT or CAM-ECT methodology. New CESM-POP simulation data to be evaluated may be the result of using a new architecture or a different compiler option, making a code modification, or changing the input data deck. pyCECT evaluates whether the new ocean model simulation results are statistically consistent with the specified POP-ECT ensemble and issues an overall "pass" or "fail" designation. In addition, the Z-score passing rate is given for each ocean model variable at the selected checkpoint time t_C.

4 Experiments

The primary objective of this section is to evaluate the new POP-ECT tool on CESM-POP simulation data with a series of experiments on configurations with expected outcomes, including revisiting the effect of changing the barotropic solver convergence tolerance as in Hu et al. (2015) and discussed in Section 2. Experiments were run with the CESM 1.2.2 release with the default Intel 13.2.1 compiler, using CESM-POP for the active ocean component, the CICE model for the active sea ice component, and data-driven atmosphere and land components. In addition, we use the climatologically-averaged atmospheric forcing (one-year repeating forcing) framework for ocean-ice simulations. Therefore, there are no year-to-year corresponding events (such as El Niño Southern Oscillation), and the variance in the equatorial Pacific may be artificially suppressed. (Note that this particular CESM component configuration is referred to in CESM documentation as a "G_NORMAL_YEAR" component set). The CESM grid resolution was "T62_g16", which corresponds to a $1°$grid (320×384) for the ocean and ice components, with 60 vertical levels and a displaced Greenland pole. Simulations were run on 96 processor cores on the Yellowstone machine at NCAR (unless otherwise specified).

For these experiments, we evaluate 36 months of data as opposed to a single time slice to provide insight as to how the ZPRs vary over time and guide the selection of t_C. Further, to illuminate the relationship between the Z-score and simulation month in terms of ZPR and guide the selection of tol_Z and min_{ZPR}, we utilize a Response Surface Methodology (RSM) (e.g., Box and Draper, 2007). That is, we provide plots of the response surfaces for variable $\tilde{X}$ where the percentage of grid points i that meet the Z-score tolerance criteria, $Z_{\tilde{x}_i} > tol_Z$, are shown with a cumulative distribution function (CDF) for a range of tol_Z values and simulation months. Finally, as noted previously, we find an ensemble size of 40 to be sufficient for our experiments, but we further explore and discuss the ensemble size parameter selection in Sect. 5.

For simplicity, we show results for temperature (TEMP) and sea surface height (SSH). Though we analyzed the other variables as well, these two are representative of the ocean system model in general as SSH is related to ocean circulation dynamics and TEMP is determined by model scalar transport.

4.1 Barotropic solver convergence tolerance

First we use the newly enhanced CESM-ECT to revisit the effect of changing the barotropic solver convergence tolerance, as discussed in Sect. 2 in reference to the work in Hu et al. (2015). The default barotropic solver convergence tolerance in CESM-POP is 10^{-13}, and we ran experiments with convergence tolerances ranging from 10^{-9} to 10^{-16}, outputting monthly temporal averages at each grid point for 36 months. We expect convergence tolerances tighter than the default 10^{-13} to result in a consistant climate, but looser tolerances to introduce some error.

Response surfaces for TEMP and SSH are given in Fig. 4 and Fig. 5, respectively. Each figure contains four response surfaces: the original default convergence tolerance (10^{-13}) and a tighter tolerance (10^{-16}) in the top two subplots and looser tolerances (10^{-10} and $5.0 * 10^{-9}$) in the bottom two subplots. For each response surface, the x-axis indicates the simulation month (ranging from 1 to 36), and the y-axis indicates the range of Z-score values used for tol_Z when calculating the percentage of grid points that fall below the Z-score tolerance, i.e. ZPR in Eq. (2) . The color bar indicates the ZPR as a percentage in

increments of 10%. The response surface plots are useful for evaluating various combinations of options for tol_Z and min_{ZPR}. For example, consider the effect on variable TEMP of modifying the solver convergence tolerance. The upper left subplot in Fig. 4 indicates that for the original convergence tolerance (10^{-13}), 90% of all grid points had a Z-score of less than 2.0 at all simulation months. In contrast, the subplot below for 10^{-10} shows that after the first 9 simulation months, 90% of the grid points have a Z-score less 3.0, and by 12 months, between 70 and 80 percent of the grid points have Z-scores less than 2.0. Further loosening the convergence tolerance to $5.0 * 10^{-9}$ as in the lower right subplot shows pronounced errors in terms of the relatively low ZPR percentages. If we turn our attention to SSH in Fig. 5 for the same four convergence tolerances, the overall trends are similar. In particular, for 10^{-13}, 90% of all grid points have a Z-score of less than 2.0 at all simulation months (except month 6). Similarly to TEMP, the subplot for 10^{-10} shows that errors have been introduced and errors are even more pronounced for $5.0 * 10^{-9}$. A notable difference between the response surfaces for TEMP and SSH is that the plots for temperature are smoother over time because diffusion is an important process in the temperature calculation.

If we fix the Z-score tolerance for the data shown in Fig. 4 and Fig. 5, we can more easily evaluate the ZPR. Consider setting $tol_Z = 3.0$, a rather conservative choice. Fig. 6 illustrates the percentage of grid points with Z-scores that exceed $tol_Z = 3.0$ (i.e. *fail*) for both TEMP and SSH. If we choose a ZPR threshold of $min_{ZPR} = 0.9$, which corresponds to a 10% Z-score failure rate in Fig. 6, it is clear that a convergence tolerance of 10^{-10} is borderline in terms of passing or failing (and therefore should not be used in practice). Whereas tolerances tighter than 10^{-10} have low Z-score failure rates and appear statistically consistent with the original tolerance for both variables. This plot in Fig. 6 is of interest as well as it nicely demonstrates that as the convergence tolerance becomes less strict, the number of grid points exceeding the Z-score tolerance increases. This result is much clearer than in Hu et al. (2015).

4.2 Processor layouts

While CESM simulations that are identical except for differing numbers of CESM-POP processor cores yield non-BFB identical results, the results from such simulations should represent the same climate state (i.e., they should not be statistically distinguishable). Here we verify that such simulations definitively pass CESM-ECT. Recall that the simulations comprising our CESM-ECT ensemble were run on 96 cores. We ran additional simulations on 48, 192, and 384 cores. Note that we are not using threading in CESM-POP at this time.

The response surface plots for 96 cores (labeled "original") and 384 cores are the top subplots in Fig. 8 and Fig. 9 for TEMP and SSH, respectively. These plots show that for both core counts, 90% of all grid points have a Z-score of less than 2.0 for nearly all simulation months, and as expected, there is little discernable difference between the two core counts for both variables. As before, we fix the Z-score tolerance at $tol_Z = 3.0$ and show the Z-score failure rates for TEMP with all four core count options (48, 96, 192, and 384) in Fig. 7. As anticipated, the Z-score failure percentages are quite low (below 1.2%) for all configurations at all monthly time slices, confirming that differences in simulation output due to varying the core count in CESM-POP are not statistically significant and correctly identified as such by the new CESM-ECT methodology. Note that the corresponding plot for SSH is not provided as is looks similarly good in terms of very low Z-score failure rates.

4.3 Physical parameters

Now we change two physical parameters expected to alter the ocean climate from the tracer equations: the tracer's vertical mixing coefficient for convective instability and the tracer advection scheme. Results from these modifications should fail the CESM-ECT. First, by default, the vertical mixing coefficient for convective instability (*convect_diff*) is set to be *convect_diff* = 10,000 for the tracer mixing coefficient in the 1°CESM-POP configuration. We increase this parameter by factors of 2, 5, and 10, which is expected to increase the vertical mixing in the ocean interior when the density profile is unstable. This should noticeably impact the CEM-POP results due to the different mixing property. Second, we change the POP tracer advection scheme (*t_advect_ctype*) from the default 3rd-order upwind scheme (*upwind3*) to the Lax-Wendroff scheme with 1D flux limiters (*lw_lim*). This change is also significant and should lead to a different climate state because the associated diffusion and dispersion errors differ.

The response surface plots for increasing *convect_diff* by a factor of 10 are given in the lower left subplots in Fig. 8 and Fig. 9 for TEMP and SSH, respectively. This change clearly affects the climate state significantly, particularly as compared to changing the CESM-POP core count to 384 as depicted in the upper right subplot in both figures. In fact, the impact on TEMP of increasing *convect_diff* in Fig. 8 is almost as strong as changing the solver convergence tolerance to 10^{-9} in Fig. 4. The change of the advection scheme also leads to different climate state, evident in the lower right subplots in Fig. 8 and Fig. 9 for TEMP and SSH, respectively. Note that the Z-scores at nearly every grid point are failing.

The Z-score failure rates for $tol_Z = 3.0$ are shown in Fig. 10 for advection scheme change as well as all the modifications to the tracer vertical mixing coefficient for convective instability. If we choose a ZPR threshold of $min_{ZPR} = 0.9$, which corresponds to a maximum of 10% Z-score failure rate, then doubling the vertical mixing coefficient (*convect_diff*2) is borderline in terms of passing or failing. The remaining tests clearly fail for both TEMP and SSH, as expected. Based on our experiments thus far, choosing a Z-score tolerance of $tol_Z = 3.0$ and a ZPR threshold of $min_{ZPR} = 0.9$ yields the expected outcome, and these parameter settings are the default for the pyCECT tool.

4.4 Simulation length

Our experiments in Fig. 10 indicate that the percentage of grid points with failing Z-scores differs little from month to month after the first 12 months for both TEMP and SSH. This conclusion can also be reached from Fig. 8 and Fig. 9 for TEMP and SSH, respectively. In particular, the response of SSH to the initial temperature perturbation is largely stabilized after 12 months. The SSH may be affected through the circulation change resulting from the change of density stratification. Based on our experimental results, evaluating the output at a single well-chosen checkpoint time t_C appears reasonable.

We generally choose $t_C = 12$ to minimize the computational requirements of creating the ensemble for each candidate CESM tag. (The ensemble simulations runs can be length t_C.) Consider the surface plots for month $t_C = 12$ in Fig. 11 that illustrate the Z-score values for SST as compared to the ensemble for four different model configurations. The top subplot is the original case. The second plot from the top is the result of changing the number of CESM-POP processor cores to 384, which resembles the topmost plot as expected. While the patterns are not identical for the upper two plots, the Z-score

magnitudes and distributions are similar, indicating a degree of statistical consistency when changing the number of processors. In contrast, increasing the tracer mixing coefficient for convective instability by a factor of 10 was shown to change the climate state in Sect. 4.3, and this result is clearly evident in the Z-score at month 12 in the third plot from the top of Fig. 11. Finally, the bottom subplot in Fig. 11 indicates a largely altered climate state due to the use of a different advection scheme, which corroborates the substantial effects seen in Fig. 8 and Fig. 9. Using a different advection scheme significantly changes the numerical dissipation and diffusion associated with the scheme (Tseng, 2008) and effectively influences the circulation pattern and structure in the ocean model (e.g., Tseng and Dietrich, 2006). In particular, the Lax-Wendroff scheme with flux limiters can introduce excessive numerical mixing which may interact with the physical mixing of temperature and salinity, though it can result in a much smoother solution in general.

4.5   Hardware and compiler modifications

A primary quality assurance responsibility of POP-ECT is to ensure that changes to either the hardware or software stack do not negatively affect POP-CESM simulation output. Here we use POP-ECT to evaluate the consistency of simulations that result for compiler or hardware modifications that lead to non-BFB results, but are not expected to be climate-changing. We run POP-ECT with the default parameters suggested in the previous subsections: $t_C = 12$, $tol_Z = 3.0$, and $min_{ZPR} = 0.9$. Results from all of these experiments are listed in Table 1, where the Z-score passing rate (ZPR) is given for all five diagnostic variables, which are described in Sect. 3.1. Note that $min_{ZPR} = 0.9$ means that POP-ECT returns a *pass* only if the ZPR is at least 0.9 for all five variables. Recall that the default compiler for CESM 1.2.2 on NCAR's Yellowstone machine is Intel 13.1.2 with -O2 optimization. The first two experiments use the same Intel compiler version but different optimizations levels: Intel 13.1.2 with -O0 and Intel 13.1.2 with -O3. The next two experiments use more recent versions of the Yellowstone Intel compiler: Intel 15.0.0 with -O2 and 16.0.2 with -O2. We then evaluate the two additional CESM 1.2.2-supported compiler configurations on Yellowstone: GNU 14.8.0 and PGI 13.9, and also evaluate a more recent version of PGI (14.7). Finally, for completeness, we run simulations on alternative CESM-supported platforms: the Edison and Cori machines located at the National Energy Research Scientific Computing Center (NERSC). Table 1 indicates that all of these simulations results *pass* the POP-CECT, with the exception of the *fail* result for PGI 13.9 on Yellowstone. The failure for PGI 13.9 suggests that some aspect of the CESM-POP code may be sensitive to this compiler version. While we have not determined why PGI 13.9 causes the discrepancy in simulation output, POP-ECT appropriately returns a *fail* as notable differences do exist between the default Intel 13.1.2 and the PGI 13.9 simulations (as compared, for example to differences between the default Intel 13.1.2 and GNU 14.8 simulations), as shown for the top-level zonal velocity (UVEL) in Fig. 12. Note, however, that results with PGI 14.7 are consistent, perhaps indicating a correction in this more recent version of PGI.

5   Ensemble size

The size (i.e., number of members) of the ensemble must be large enough to sufficiently capture ocean model variability, but as small as possible for computational efficiency. In this section, we discuss the sensitivity of POP-ECT to ensemble size. We

setup experiments to determine the false positive rate associated with multiple ensembles sizes as follows. First, we generate a total of 80 ensemble members that differ by an $\mathcal{O}(10^{-14})$ perturbation to the initial ocean temperature field. Second, from the 80 members, we remove 10 to use as our test set. Next, from the remaining 70 members, we create ensembles of sizes 10, 20, 30, 40, 50, and 60. In particular, for each ensemble size, we do 100 random draws for each ensemble size from the

5   set of 70 members, resulting in 100 distinct ensembles corresponding to each ensemble size. Then for each ensemble size, we run POP-ECT at $t_c = 12$ months for each of the 10 members of the test set with all 100 ensembles of that size, resulting in 1000 tests per ensemble size. We consider the measured experimental failure rate to be the type I error, or "false positive" rate. Because the test set and the ensemble members are all drawn from the larger 80 member collection that represents a statistically consistent climate, the Z-score failure rate would ideally be as low as possible.

10   Figure 13 shows the results of performing these experiments for variables TEMP and SSH. The x-axis indicates the ensemble size, and the y-axis indicates the Z-score failure rate. For each ensemble size, the squares denote the mean and the error bars indicate one standard deviation of uncertainty. As expected, as the ensemble size increases, the false positive rate decreases and the range of uncertainty shrinks. However, increasing the ensemble size has diminishing returns; the improvement in false positive rate when using 20 instead of 10 members is much greater than the improvement gained by using 60 instead of 50

15   members. We choose an ensemble size of 40 as improvement beyond that is marginal and we balance a low false positive rate with keeping the cost of the ensemble generation low.

6   Conclusions and Future Work

Because the CESM-POP ocean model is widely-used and critical to many climate simulations, assuring its quality is of paramount importance. However, the chaotic nature of ocean dynamics often leads to simulation results that are not identical in

20   the presence of minor differences, such as a change in processor core count for the simulation. Therefore, the ability to easily determine whether differences in model results are statistically significant is important to both climate scientists and model developers. The ensemble methodology developed for evaluating consistency with atmospheric data, CAM-ECT, was not appropriate for ocean simulation data based on its differing characteristics. Therefore, we developed a new ocean model-specific methodology for statistical consistency testing, POP-ECT, that allows for the subjective detection of statistically significant

25   changes in CESM-POP. Together with the new methodology, using an appropriately-sized ensemble is critical as well. Our experiments indicate the appropriateness of the new approach for detecting differences in the model ocean state. The addition of POP-ECT to the CESM-ECT suite of tools has greatly enhanced the capability to ensure quality CESM simulations in the midst of the on-going state of CESM development and continually evolving hardware and software environments.

      We plan to extend this work in a number of ways. First, the existing spatial approach lends itself to the examination of

30   regional ocean diagnostics. For example, named oceans could be identified individually as the source of failure if the global test fails. Enabling the move from coarse- to fine-grain diagnostics would facilitate determining the root cause of an error or difference. Second, we plan to extend the evaluation of the effects of data compression on climate data in Baker et al. (2014) to ocean model data and will use the testing methodology presented here to evaluate the impact. The ability to determine whether

changes in the ocean state are statistically significant or not due to data loss during compression is critical to the acceptance of compression as a tool to reduce data volumes for ocean simulation data.

7 Code availability

The CESM-ECT Python tools (pyCECT v2.0) can be obtained independently of CESM from NCAR's public git repository (https://github.com/NCAR/PyCECT/releases). The version of CESM used for our experiments, CESM 1.2.2, is available at http://www.cesm.ucar.edu/models/cesm1.2. The CESM-ECT software tools are also included in the CESM public releases, with the POP-ECT addition available starting with the CESM 2.0 release series. CESM-POP simulation data is available from the corresponding author upon request.

Acknowledgements. This research used computing resources provided by the Climate Simulation Laboratory at NCAR's Computational and Information Systems Laboratory (CISL), sponsored by the National Science Foundation and other agencies. This research used resources of the National Energy Research Scientific Computing Center, a DOE Office of Science User Facility supported by the Office of Science of the U.S. Department of Energy under Contract No. DE-AC02-05CH11231. This work is supported in part by a grant from the National Natural Science Foundation of China (41375102) and the National Grand Fundamental Research 973 Program of China (No. 2014CB347800).

References

Baker, A. H., Xu, H., Dennis, J. M., Levy, M. N., Nychka, D., Mickelson, S. A., Edwards, J., Vertenstein, M., and Wegener, A.: A Methodology for Evaluating the Impact of Data Compression on Climate Simulation Data, in: Proceedings of the 23rd International Symposium on High-performance Parallel and Distributed Computing, HPDC '14, pp. 203–214, 2014.

Baker, A. H., Hammerling, D. M., Levy, M. N., Xu, H., Dennis, J. M., Eaton, B. E., Edwards, J., Hannay, C., Mickelson, S. A., Neale, R. B., Nychka, D., Shollenberger, J., Tribbia, J., Vertenstein, M., and Williamson, D.: A new ensemble-based consistency test for the Community Earth System Model, Geoscientific Model Development, 8, 2829–2840, doi:10.5194/gmd-8-2829-2015, 2015.

Box, G. E. P. and Draper, N. R.: Response Surfaces, Mixtures, and Ridge Analyses, Second Edition, John Wiley and Sons, 2007.

Carson, II, J. S.: Model Verification and Validation, in: Proceedings of the 2002 Winter Simulation Conference, pp. 52–58, 2002.

Clune, T. and Rood, R.: Software Testing and Verification in Climate Model Development, IEEE Software, 28, 49–55, doi:http://dx.doi.org/10.1109/MS.2011.117, 2011.

Easterbrook, S. M., Edwards, P. N., Balaji, V., and Budich, R.: Guest Editors' Introduction: Climate Change - Science and Software, IEEE Software, 28, 32–35, 2011.

Hu, Y., Huang, X., Baker, A. H., Tseng, Y., Bryan, F. O., Dennis, J. M., and Yang, G.: Improving the scalability of the ocean barotropic solver in the Community Earth System Model, in: Proceedings of the International Conference for High Performance Computing, Networking, Storage and Analysis, SC '15, pp. 42:1–42:12, doi:10.1145/2807591.2807596, http://doi.acm.org/10.1145/2807591.2807596, 2015.

Hurrell, J. W., Holland, M. M., Gent, P. R., Ghan, S., Kay, J. E., Kushner, P. J., Lamarque, J. F., Large, W. G., Lawrence, D., Lindsay, K., Lipscomb, W. H., Long, M. C., Mahowald, N., Marsh, D. R., Neale, R. B., Rasch, P., Vavrus, S., Vertenstein, M., Bader, D., Collins, W. D., Hack, J. J., Kiehl, J., and Marshall, S.: The Community Earth System Model: A Framework for Collaborative Research, Bulletin of the American Meteorological Society, 94, 1339–1360, doi:10.1175/BAMS-D-12-00121.1, 2013.

Legeckis, R.: Long waves in the eastern equatorial Pacific: A view from geostationary satellite., Science, 196, 1177–1181, 1977.

Oberkamf, W. and Roy, C.: Verification and Validation in Scientific Computing, Cambridge University Press, 13-51, 2010.

Pipitone, J. and Easterbrook, S.: Assessing climate model software quality: a defect density analysis of three models, Geoscientific Model Development, 5, 1009–1022, doi:10.5194/gmd-5-1009-2012, 2012.

Smith, R., Jones, P., Briegleb, B., Bryan, F., Danabasoglu, G., Dennis, J., Dukowicz, J., Fox-Kemper, C. E. B., Gent, P., Hecht, M., et al.: The Parallel Ocean Program (POP) Reference Manual Ocean Component of the Community Climate System Model (CCSM), 2010.

Steele, M., Morley, R., and Ermold, W.: PHC: A global ocean hydrography with a high-quality Arctic Ocean, Journal of Climate, 14, 2079–2087, 2001.

Stocker, T., Qin, D., Plattner, G., Tignor, M., Allen, S., Boschung, J., Nauels, A., Xia, Y., Bex, B., and Midgley, B.: IPCC, 2013: Climate Change 2013: the physical science basis. Contribution of working group I to the fifth assessment report of the Intergovernmental Panel on Climate Change, 2013.

Tseng, Y.-H.: High-order essentially local extremum diminishing schemes for environmental flows, International Journal for Numerical Methods in Fluids, 58, 213–235, doi:10.1002/fld.1725, 2008.

Tseng, Y.-H. and Dietrich, D. E.: Entrainment and Transport in Idealized Three-Dimensional Gravity Current Simulation, Journal of Atmospheric and Oceanic Technology, 23, 1249–1269, 2006.
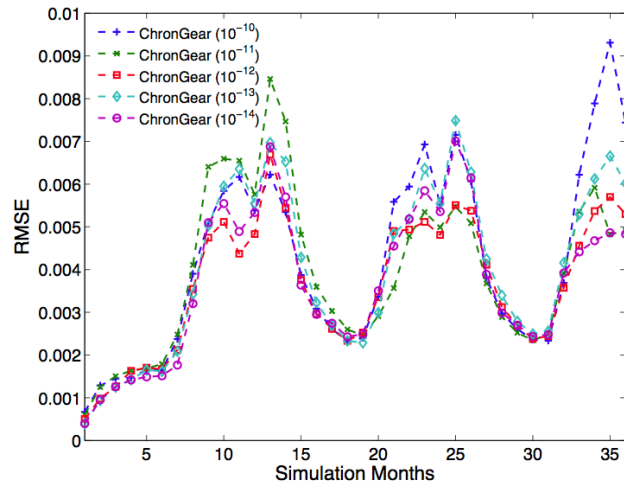
Figure 1. Monthly Root Mean Square Error (RMSE) of temperature for experiments with different barotropic solver convergence tolerances. Note that this is a subset of Fig. 12 in Hu et al. (2015).
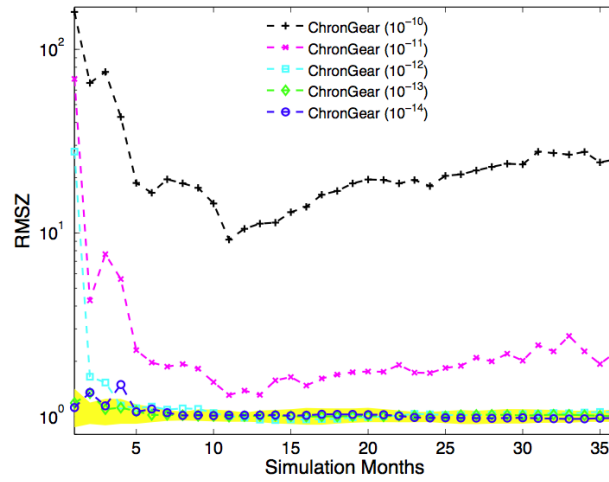
Figure 2. Monthly Root Mean Square Z-score (RMSZ) of temperature with respect to an ensemble (denoted by yellow) for experiments with barotropic different convergence tolerances. Note that this is subset of Fig. 13 in Hu et al. (2015).
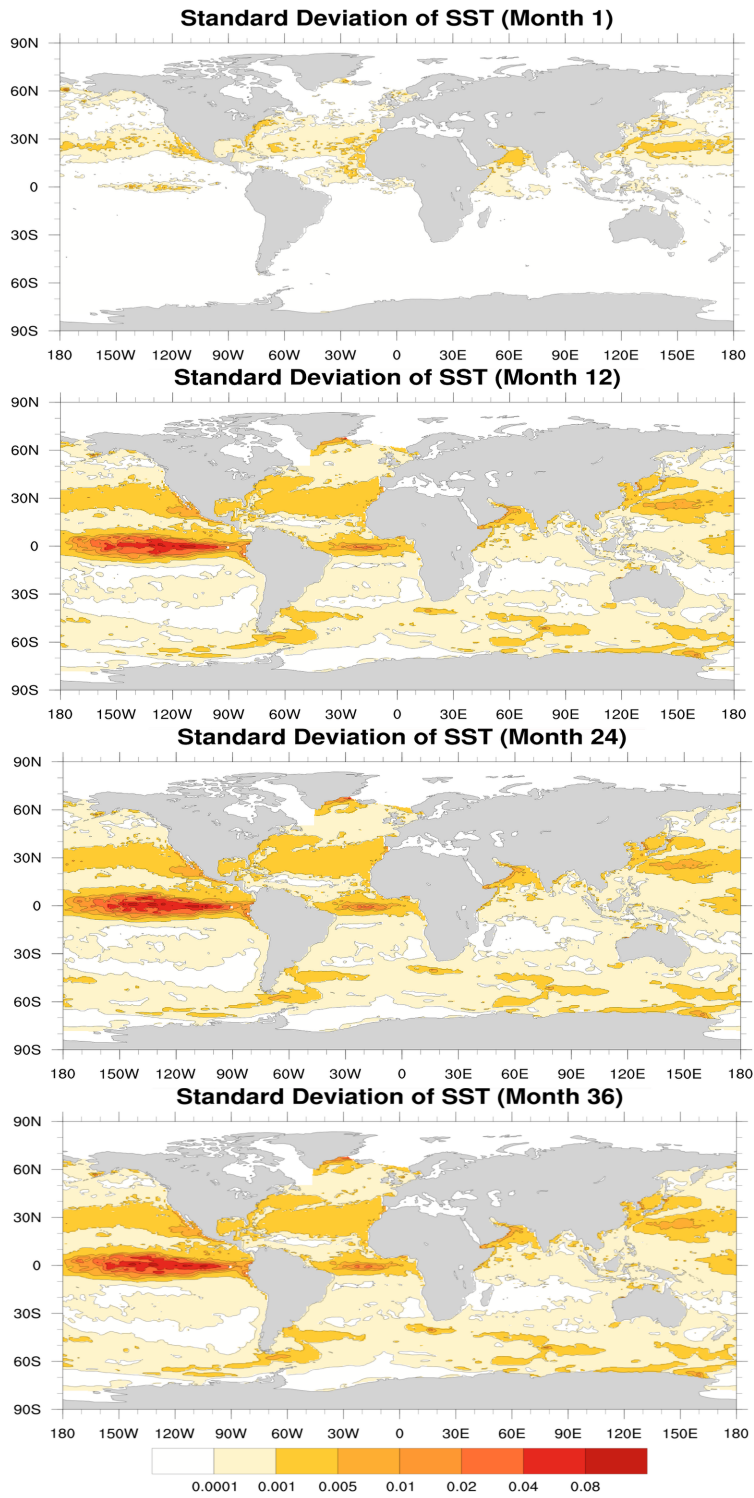
Figure 3. The ensemble distribution for the standard deviation of sea surface temperature (SST) at months 1, 12, 24, and 36.
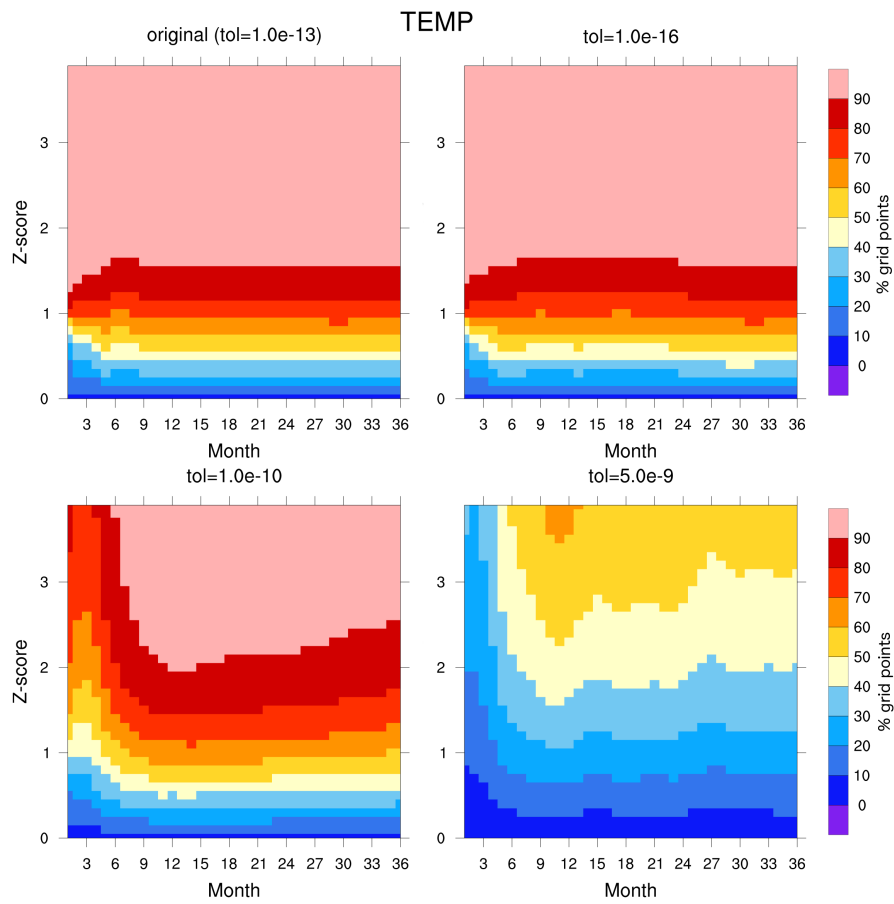
Figure 4. Response surfaces for Z-score of temperature (TEMP) over time (monthly) and Z-score tolerance. Each subplot represents a different barotropic solver convergence tolerance (labeled above). The color bar indicates the percentage of grid points with a Z-score below the Z-score tolerance (on the y-axis).
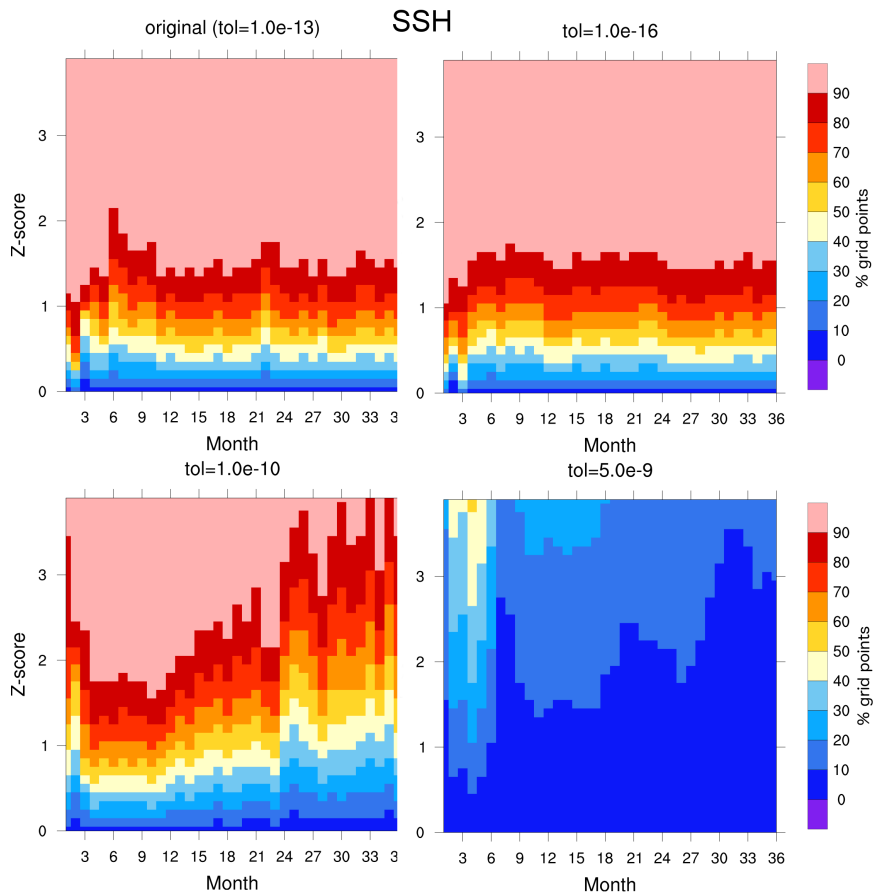
Figure 5. Response surface for Z-score of sea surface height (SSH) over time (monthly) and Z-score tolerance. Each subplot represents a different barotropic solver convergence tolerance (labeled above). The color bar indicates the percentage of grid points with a Z-score below the Z-score tolerance (on the y-axis).
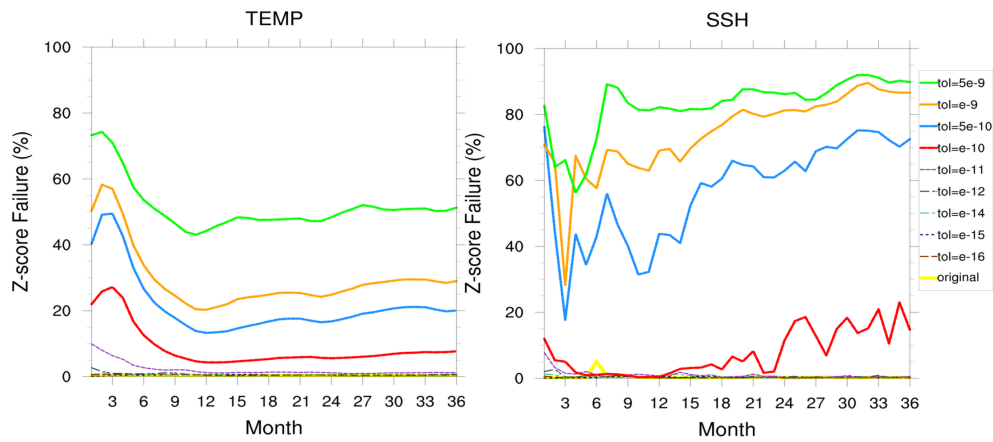
Figure 6. Percentage of grid points with Z-scores for temperature (TEMP) and sea surface height (SSH) that exceed the 3.0 tolerance for simulations with various barotropic solver convergence tolerances.
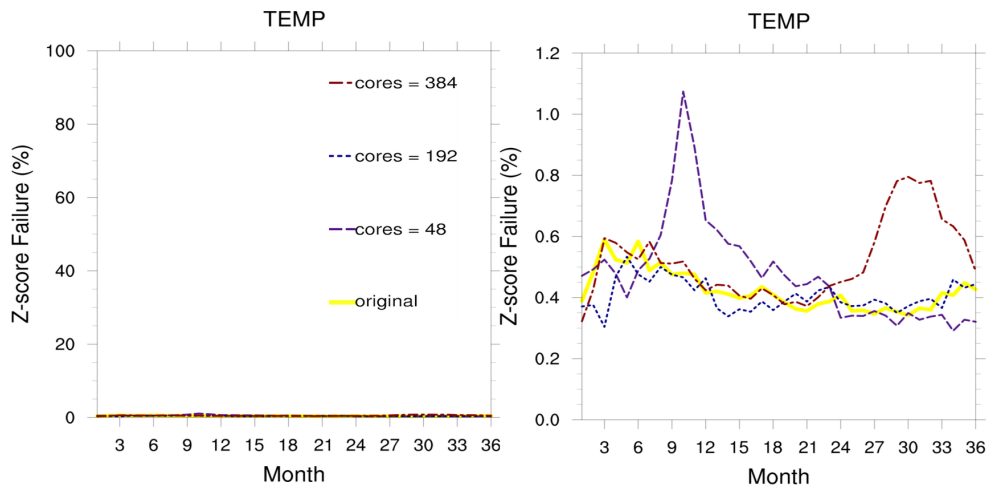
Figure 7. Percentage of grid points with Z-scores for temperature (TEMP) that exceed the 3.0 tolerance for simulations with various numbers of processor cores. (Note that the left and right subplots contain the same information, with different scales for the y-axis.)
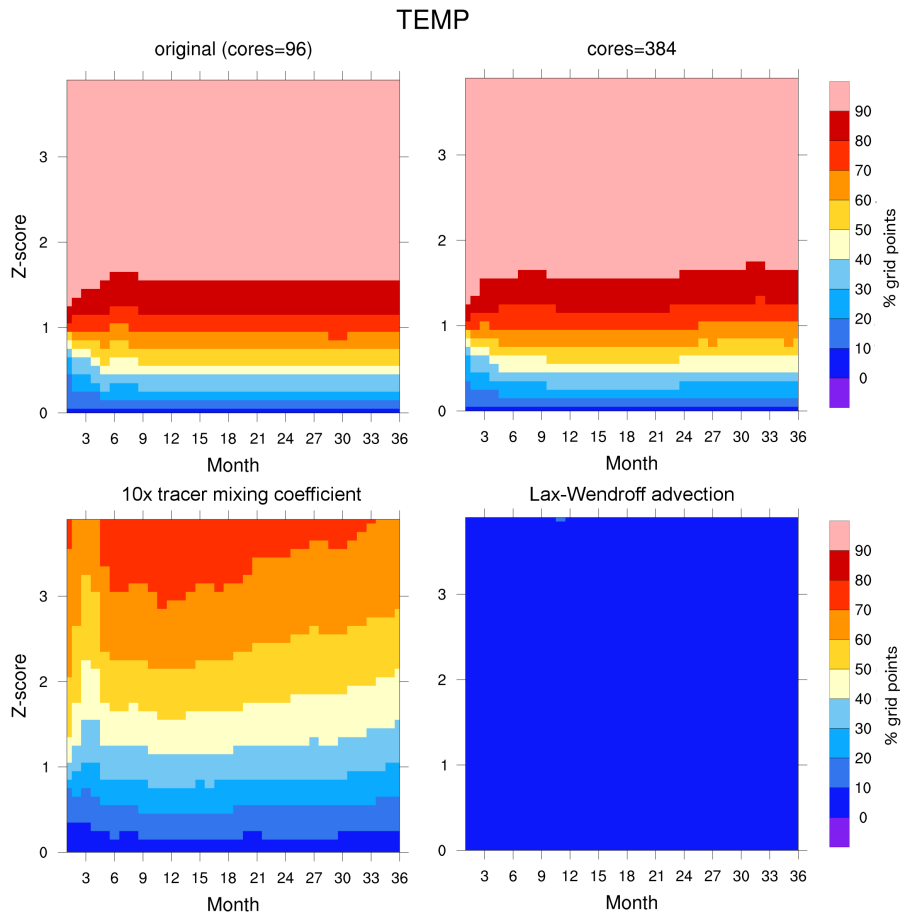
Figure 8. Response surfaces for Z-score of temperature (TEMP) over time (monthly) and Z-score threshold. The top two subplots represent two different processor core layouts. The bottom left has a tracer mixing coefficient for convective instability that is 10 times larger than the original (100000.0), and the bottom right uses a different tracer advection scheme (Lax-Wendroff scheme with 1D flux limiters). The color bar indicates the percentage of grid points with a Z-score below the Z-score tolerance (on the y-axis).
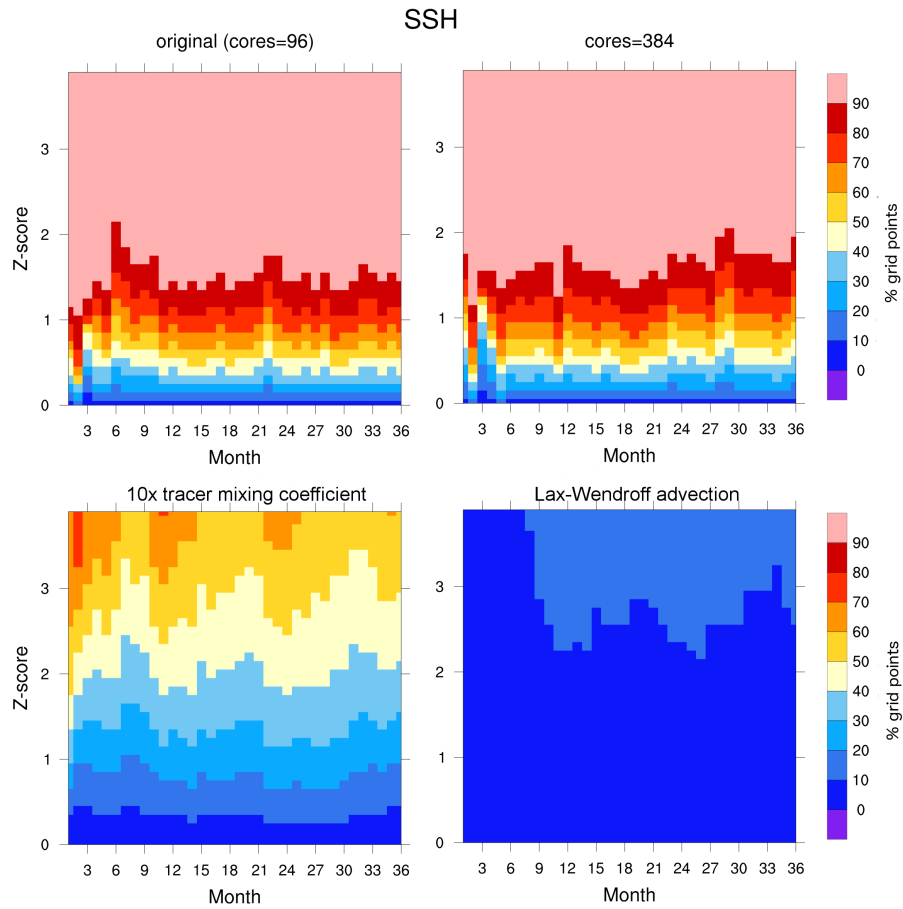
Figure 9. Response surfaces for Z-score of sea surface height (SSH) over time (monthly) and Z-score threshold. The top two subplots represent two different processor core layouts. The bottom left has a tracer mixing coefficient for convective instability 10 times larger than the original (100000.0), and the bottom right uses a different tracer advection scheme (Lax-Wendroff scheme with 1D flux limiters). The color bar indicates the percentage of grid points with a Z-score below the Z-score tolerance (on the y-axis).
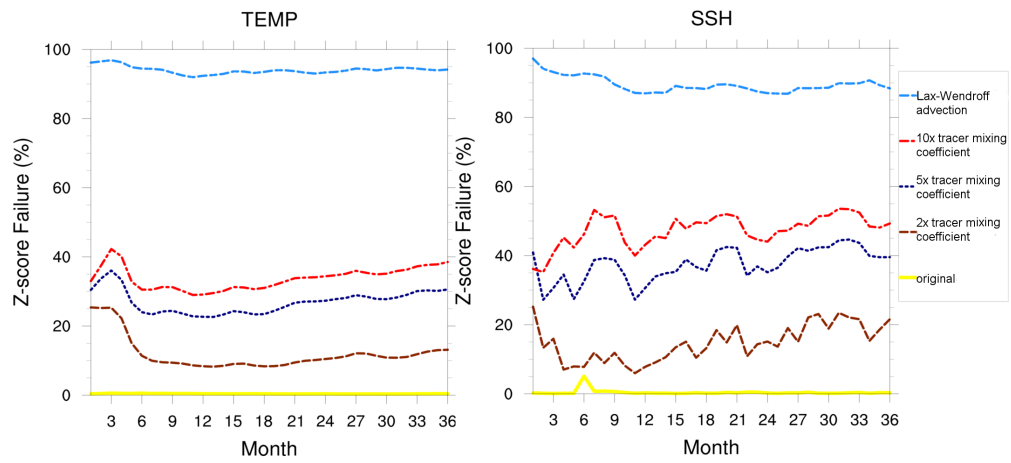
Figure 10. Percentage of grid points with Z-scores for temperature (TEMP) and sea surface height (SSH) that exceed the 3.0 threshold for simulations with an alternative tracer advection scheme (lw_lim) and several tracer mixing coefficients for convective instability.
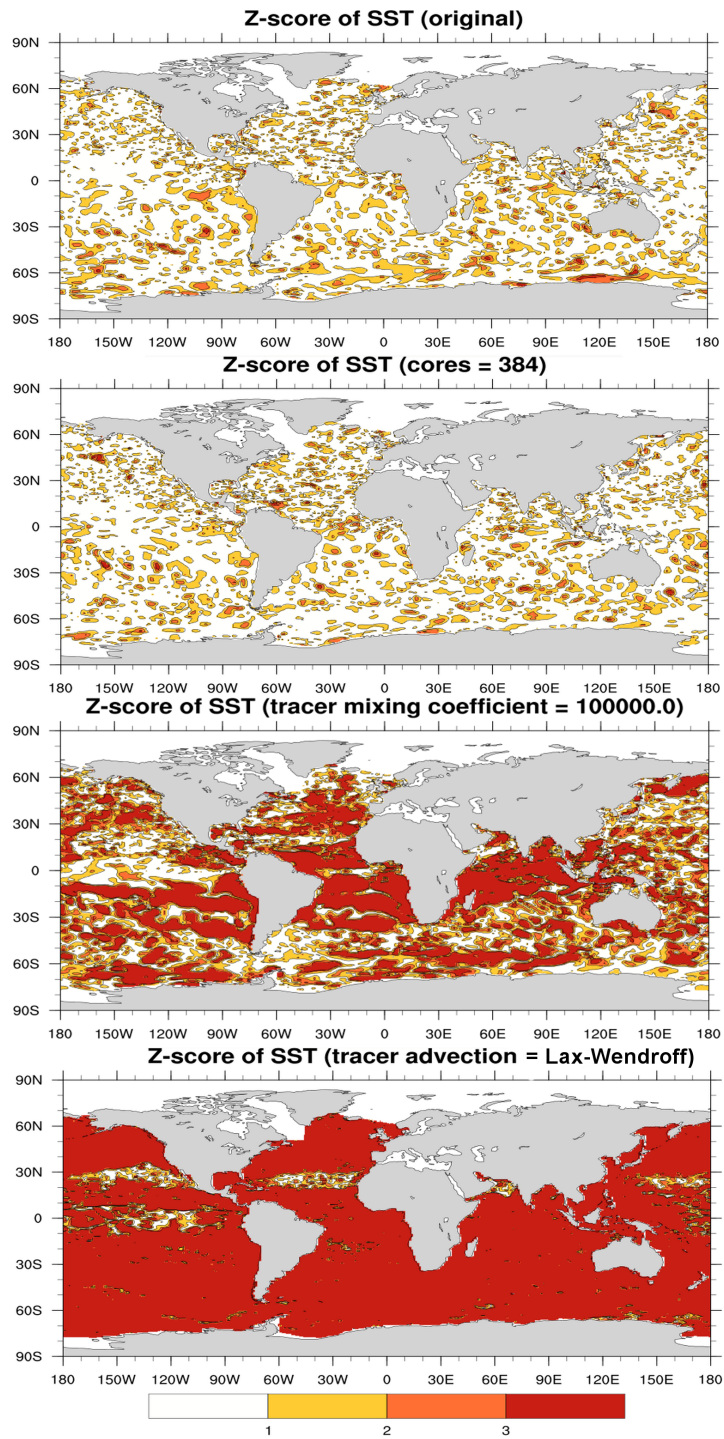
Figure 11. Z-score of sea surface temperature (SST) at month 12 for the original (default) case, a 384 processor core case, a case with a 10 times larger tracer mixing coefficient for convective instability (100000.0), and a case with an alternate tracer advection scheme (Lax-Wendroff scheme with 1D flux limiters).

Table 1. Z-score passing rate (ZPR) for POP-ECT with default parameters $t_C = 12$, $tol_Z = 3.0$, and $min_{ZPR} = 0.9$ for each of the 5 diagnostic variables (described in Section 3.1). Note that the top 7 experiments all use NCAR's Yellowstone machine.

Experiment	POP-ECT result	UVEL	VVEL	TEMP	SALT	SSH
				Z-score passing rate		
Intel 13.1.2 -O0	PASS	0.988	0.988	0.989	0.992	0.992
Intel 13.1.2 -O3	PASS	0.995	0.995	0.994	0.994	0.996
Intel 15.0.0 -O2	PASS	0.988	0.988	0.989	0.992	0.992
Intel 16.0.2 -O2	PASS	0.993	0.993	0.993	0.994	0.995
GNU 14.8.0	PASS	0.993	0.994	0.994	0.996	0.992
PGI 13.9	FAIL	0.073	0.088	0.004	0.006	0.002
PGI 14.7	PASS	0.995	0.995	0.994	0.995	0.996
Edison machine (NERSC): Intel 16.0.0.109	PASS	0.995	0.995	0.994	0.995	0.996
Cori machine (NERSC): Intel 16.0.0.109	PASS	0.993	0.995	0.994	0.996	0.997
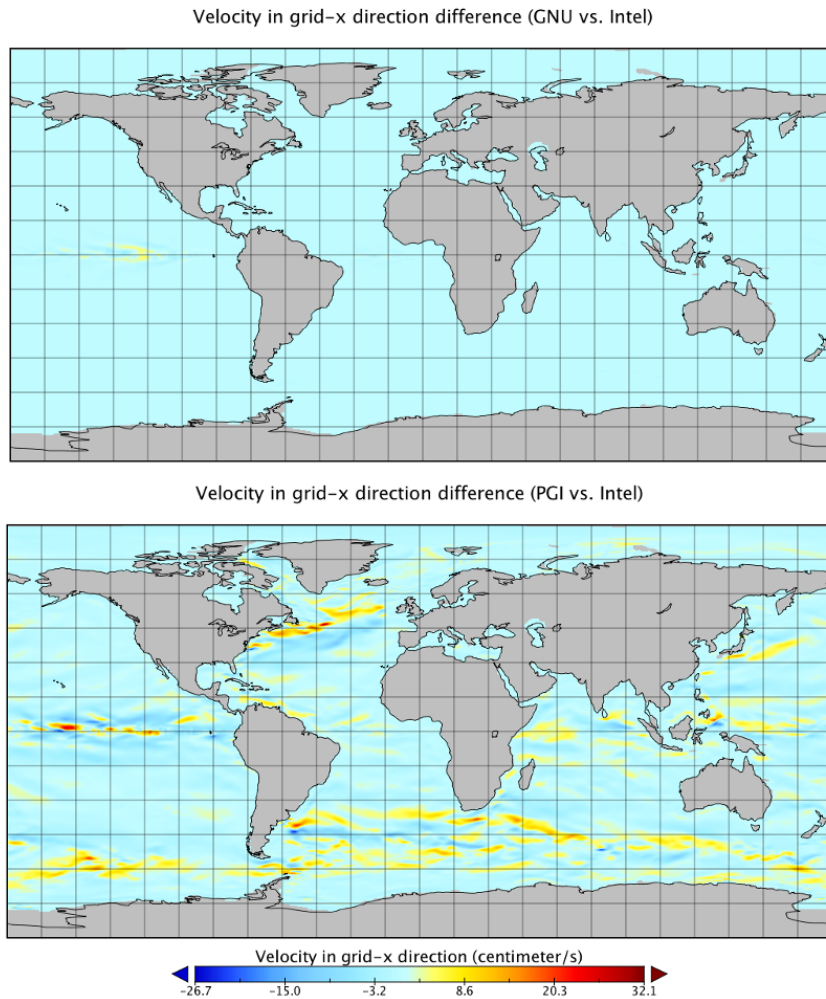
Figure 12. Differences in the top-level zonal velocity (UVEL) in cm/s at month 12. The top plot shows the differences between the GNU 14.8 and default Intel simulation ouput. The lower plot shows the differences between PGI 13.9 and the default Intel 13.1.2 simulation outputs. Note that the min, max, and mean data values for UVEL for the default Intel 13.1.2 simulations at month 12 (top-level) are -80.9, 77.0, and -0.8 cm/s, respectively. For comparison, the min, max, and mean data values for UVEL are -87.9, 69.8 and -0.9 cm/s for the PGI 13.9 simulation data.
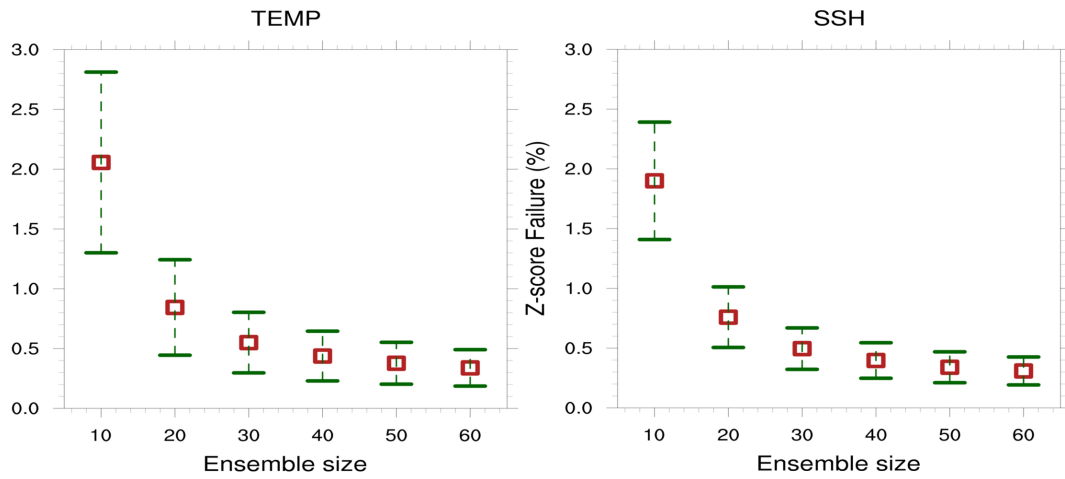
Figure 13. The distributions of experimental failure rates based on 1000 tests for variables temperature (TEMP) and sea surface height (SSH). For each ensemble size, the green bars indicate the maximum and minimum values obtained, and the red boxes indicate the mean.